J. Phase Equilib. Diffus. (2020) 41:538–549
https://doi.org/10.1007/s11669-020-00823-3

Predicting Feasible Modifications of Ce_2ON_2 Using a Combination of Global Optimization and Data Mining

J. Zagorac[1,2] · J. C. Schön[3] · B. Matović[1,2] · T. Škundrić[1] · D. Zagorac[1,2]

Submitted: 19 December 2019 / in revised form: 16 June 2020 / Published online: 6 July 2020

Abstract Using a combination of global optimization and data mining, we identify feasible modifications of an ionic Ce-O-N ceramic compound, with composition Ce_2ON_2, that should at least be metastable at $T = 0$ K. The energy landscape of Ce_2ON_2 has been explored for various pressures using empirical potentials followed by ab initio level optimizations, and a multitude of structure candidates has been analyzed. The structure of the energetically lowest modification among these candidates at standard pressure, α-Ce_2ON_2, is predicted to be similar to the $AlCo_2Pr_2$ structure type.

Keywords Ce-O-N compounds · computational studies · data mining · global optimization · structure prediction

1 Introduction

An important method for controlling the properties of oxide photocatalysts and tuning their band gaps is nitrogen doping.[1] Similarly, stoichiometric oxynitrides can have useful optical properties such as photocatalytic TaON[2] and yellow–red pigments in the solid solution series $CaTaO_2N$-$LaTaON_2$.[2] Furthermore, incorporation of nitrogen into ZrO_2 has been reported as an alternative method for cation doping that increases the anion vacancy concentration and stabilizes the cubic or tetragonal form at room temperature.[3] The nitrogen doped oxides show good mechanical, catalytical, and optical properties and have been reported as superionic conductors.[3]

Another important ceramic material is pure ceria (CeO_2), which has important technological applications, e.g., as catalysts, in electrolyte solid oxide fuel cells, oxygen storage components, mechanical polishing for

This invited article is part of a special tribute issue of the *Journal of Phase Equilibria and Diffusion* dedicated to the memory of Günter Effenberg. The special issue was organized by Andrew Watson, Coventry University, Coventry, United Kingdom; Svitlana Iljenko, MSI, Materials Science International Services GmbH, Stuttgart, Germany; and Rainer Schmid-Fetzer, Clausthal University of Technology, Clausthal-Zellerfield, Germany.

Electronic supplementary material The online version of this article (https://doi.org/10.1007/s11669-020-00823-3) contains supplementary material, which is available to authorized users.

✉ J. C. Schön
C.Schoen@fkf.mpg.de

J. Zagorac
jelena@vinca.rs

B. Matović
mato@vinca.rs

T. Škundrić
tamara.skundric@vinca.rs

D. Zagorac
dzagorac@vinca.rs

[1] Materials Science Laboratory "VINČA" Institute of Nuclear Sciences - National Institute of the Republic of Serbia, University of Belgrade, Belgrade, Serbia

[2] Center for Synthesis, Processing and Characterization of Materials for Application in the Extreme Conditions-CextremeLab, Belgrade, Serbia

[3] Max Planck Institute for Solid State Research, Heisenbergstr. 1, 70569 Stuttgart, Germany

microelectronics, metallurgy and biomedicine.[4-9] Doping of ceria with nonmetals is extremely rare, but it has been reported before, where the doping significantly changes the physical and chemical properties of ceria.[10-12] Besides doping with nitrogen, ceria has been doped with carbon, phosphorus, sulfur, magnesium, lanthanum, europium and praseodymium.[13-16] Similarly, cerium nitride (CeN) is a material with interesting optical, electronic and magnetic properties, related to the structure and oxidation state.[17-19] Clearly, finding a stable ionic Ce-O-N ceramic compound would be very interesting from a scientific and technological point of view, especially since this kind of material might possess many of the advanced properties mentioned above.

However, identifying (meta)stable Ce-O-N compounds accessible to an experimental synthesis is not straightforward due to the fact that cerium forms compounds with two different oxydation states (+III) and (+IV), as well as with mixed valence. In the literature there exists only one known Ce-O-N compound, $Ce(NO)_3$ containing the complex anion $(NO)^{1-}$, which crystallizes in the monoclinic *C*2/*c* space group (no. 15).[20,21] However, cerium is in the oxidation state (+III) in this compound. One of the most common compounds with cerium in the oxydation state (+IV) is pure ceria, CeO_2, exhibiting cubic symmetry (*Fm*-3*m*, no. 225) and fluorite type of structure.[22,23] Another common pure oxide of cerium is Ce_2O_3, containing Ce in oxydation state (+III); here, we also find Ce^{4+}/Ce^{3+} mixed valence compounds, depending on physical parameters such as temperature, the presence of other ions and the partial pressure of oxygen.[24,25] Similarly, CeN is a common nitride of cerium having Ce in oxydation state (+III), as well as Ce^{4+}/Ce^{3+} mixed valence,[17] with cubic symmetry (*Fm*-3*m*, no. 225) and a rock salt type of structure.[26]

In this study, we focus on one specific composition in the Ce-O-N system, the not-yet-synthesized ionic cerium oxynitride Ce_2ON_2 compound, predicting its structure using a two-pronged approach of global exploration of its energy landscape and data mining. Both methods find the same lowest energy structure, suggesting that we have been able to identify a feasible at least metastable Ce_2ON_2 ceramic compound, which should be accessible to synthesis.

2 Computational Details

To predict possible (meta)stable structure candidates in the not-yet-explored Ce_2ON_2 system, a two-pronged approach has been used, combining global optimization and data mining; details about previous successful combinations of these methods can be found elsewhere.[27-29] In the first stage of the study, we have performed a global search of the energy landscape—actually: the (potential) enthalpy landscape ($H_{pot} = E_{pot} + pV$),—of the Ce_2ON_2 compound for several pressures using simulated annealing[30] as a global optimization algorithm, followed by local optimization of the obtained candidates. Specifically, the standard stochastic simulated annealing based on random Monte Carlo walks on the energy landscape (in total 144 runs, with $4 \cdot 10^6$ steps each), was supplemented by periodic stochastic quenches (i.e. random walks with temperature $T = 0$ K) of length 3000 steps each, from 100 stopping points along every simulated annealing trajectory, as implemented in the G42+ code.[31,32] These global searches were performed for one (2 Ce, 1 O, 2 N), two (4 Ce, 2 O, 4 N), and three (6 Ce, 3 O, 6 N) formula units per variable periodically repeated simulation cell, for six different pressures (0, 0.016, 0.16, 1.6, 16, and 160 GPa). The random walk consisted of the following moves (% of Monte Carlo steps): random shifts or exchanges of atoms while keeping the cell fixed (75%), and random changes of cell parameters with (10%) or without (15%) co-moving atoms. Here, co-moving indicates that the fractional coordinates of the atoms are kept fixed while changing the cell parameters (and thus the Cartesian coordinates of the atoms change within the simulation cell), while during cell changes without co-moving atoms the Cartesian coordinates of the atoms are kept fixed within the cell and only empty slices are removed from the cell. In order to be able to perform the global searches with a reasonable computational effort, we have employed a fast computable robust empirical two-body potential consisting of Lennard-Jones ($\varepsilon = 0.3$ eV/atom; $\sigma_{ij} = (r_i + r_j)$, with effective radii r(Ce(IV)) = 1.28 Å, r(O(−II)) = 1.45 Å, and r(N(−III)) = 1.54 Å) and exponentially damped (factor: $\exp(-\mu r)$; $\mu = 0.1$/Å) Coulomb terms.[33] The epsilon parameter in the LJ-potential and the effective radii and the damping factor were taken from preliminary test runs for the binary compounds CeO_2 and CeN.

In the next step, we have performed data mining based explorations of the ICSD database,[34,35] in order to find possible structure candidates in the unknown Ce_2ON_2 system via analogy to known crystallographic structures. The reason for supplementing the global landscape exploration with a data-mining search for structure candidates is the fact that the global optimization is not assured of identifying all feasible candidates. Besides computation time limitations of the search algorithm, this is mainly due to the use of an empirical potential as energy function: Experience has shown, that on empirical energy landscapes important candidate structures may not be represented as large low-energy minima (of the kind a typical global optimization method would be designed to identify), even though they would be prominently present on an ab initio

energy landscape. On the other hand, the past thirty years have shown that many of the most relevant structure candidates (from our experience more than 50%) in a given chemical system exhibit a structure that is very similar to the crystal structure of some other compound observed in another chemical system (even if there is no obvious chemical relationship between these two chemical systems). Thus, data mining can serve as an important supplementary tool when trying to identify promising compounds in not-yet-synthetically explored chemical systems.

We have used the well-known KDD (knowledge discovery in databases) process, which involves selection, preprocessing, transformation, and interpretation/evaluation (or post-processing). In order to identify a sufficiently large number of structure candidates for the Ce_2ON_2 system, we have extracted all candidates with general formula A_2BC_2 that occur in the ICSD database,[34,35] followed by a prototype[36] analysis to reduce the plethora of candidates to a manageable number of distinct structure types. More details about the KDD process, and the combination of data mining with ab initio methods can be found elsewhere,[28,37,38] and in section 3.2.

Finally, density functional theory (DFT) ab initio calculations of the total energy, and local optimizations (including the cell parameters) of the structure candidates that had been identified during the global search with empirical potential or via data mining, were performed using the CRYSTAL17 code,[39] which is based on linear combinations of atomic orbitals. For the local optimization runs, we have employed analytical gradients.[40,41] Local optimizations are performed on the density functional theory level using the local density approximation (LDA). In the case of Ce^{4+} a pseudopotential[42] was used, together with a [*4s4p2d3f*] basis set, for O^{2-} a [*4s3p*] basis set was used,[43,44] and for N^{3-} [*3s2p*] an all-electron basis set based on Gaussian-type orbitals was employed.[45,46] The symmetries of the analyzed structures were determined using the SFND[47] and RGS[48] algorithms implemented in the program KPLOT.[49] Structures were visualized using the Vesta software.[50]

3 Results and Discussion

3.1 Global Searches and Energy Landscapes

Global searches were performed on the enthalpy landscapes for three numbers of formula units per simulation cell (Z = 1, 2, 3), and for six different pressures (0, 0.016, 0.16, 1.6, 16 and 160 GPa), yielding a total of 14,400 structure candidates. All of these structures were subjected to detailed statistical, structural, and crystallographic analysis, before submitting the most promising ones for local optimization on ab initio level.

Table 1 presents the results of the global searches performed at various pressures for 1 formula unit (Z = 1) of Ce_2ON_2. After detailed analysis we have observed that most of the local minima correspond to structure candidates that crystallize in structures containing defects or strongly distorted coordination polyhedra, exhibiting space group *P1* (no. 1). However, the empirical potential enthalpy landscape of Ce_2ON_2 with Z = 1 also contains a large variety of structure candidates with higher symmetry, at various pressures, ranging structurally from triclinic and monoclinic, to orthorhombic and tetragonal structures. The structure candidates with the lowest total energy (calculated using empirical potentials) show space group *C*2/*m* (no. 12). After further structure optimization on DFT level, these structures converted to a modification we denote as α-Ce_2ON_2 with space group *P*-3*m*1 (no.164). More details will be presented in section 3.3. However, here we note that since the α-modification exhibits the lowest total energy at both empirical and ab initio levels, the empirical potential appears to be quite suitable for describing the ionic compound Ce_2ON_2, and it is quite likely that we have identified the global energy minimum in the Ce_2ON_2 system.

It is interesting to note that with the increase of pressure, the number of distorted/defect structures decreases; at extremely high pressures of 160 GPa, the preferred modification is a tetragonal structure with space group *P*4*m*2 (no. 115). This structure is energetically favorable at empirical potential level, suggesting a phase transition might occur at high pressures. In this context, one should note that all our calculations refer to T = 0 K, and thus only the enthalpy and not the free enthalpy is used to judge the quality and relative stability of the candidates. After local ab initio optimization, the candidate structure remains in the original space group and is still energetically quite favorable; this structure has been denoted the δ-Ce_2ON_2 modification. The next interesting candidate at empirical potential level exhibits space group *Immm* (no. 71). After DFT structure optimization this structure remains in the original space group; however, energetically it is higher on ab initio level compared to other structure candidates. Still, most of the structure candidates with space groups *C*2 (no.5), *Pm* (no.6), and *Imm*2 (no.44) converted, after the local optimization, into space group *Immm* (no. 71). This suggests that this candidate represents a large local multi-minima basin—at least on empirical potential level -, which we have denoted as the Ce_2ON_2-*nf*-1 modification. This structure is visualized in Fig. 1(a) with unit cell parameters of a = 3.45 Å; b = 3.19 Å; c = 12.76 Å. Cerium is in 7-fold coordination (with atom–atom distances of 2 × 2.39 Å—O, 4 × 2.41 Å—N, 1 × 2.26 Å—N), where

Table 1 The number of structures exhibiting a certain space group found after crystallographic analysis of the results of the global searches on the empirical energy landscapes performed at various pressures for 1 formula unit ($Z = 1$) of Ce_2ON_2, before local ab initio optimization

Pressure, GPa	Space group (no.)												
	1	2	3	5	6	8	12	25	38	44	71	115	139
0	594	18	1	50	55	21	25	1	12			22	1
0.016	597	21	1	39	52	15	33	5	8	1		28	
0.16	588	29	3	42	57	28	23	4	7		1	17	1
1.6	570	23		56	52	22	35	5	12	4		21	
16	564	23	1	49	78	15	17	13	11	2	2	25	
160	494	5	1	7	49	10	4	33	4	1	4	187	1

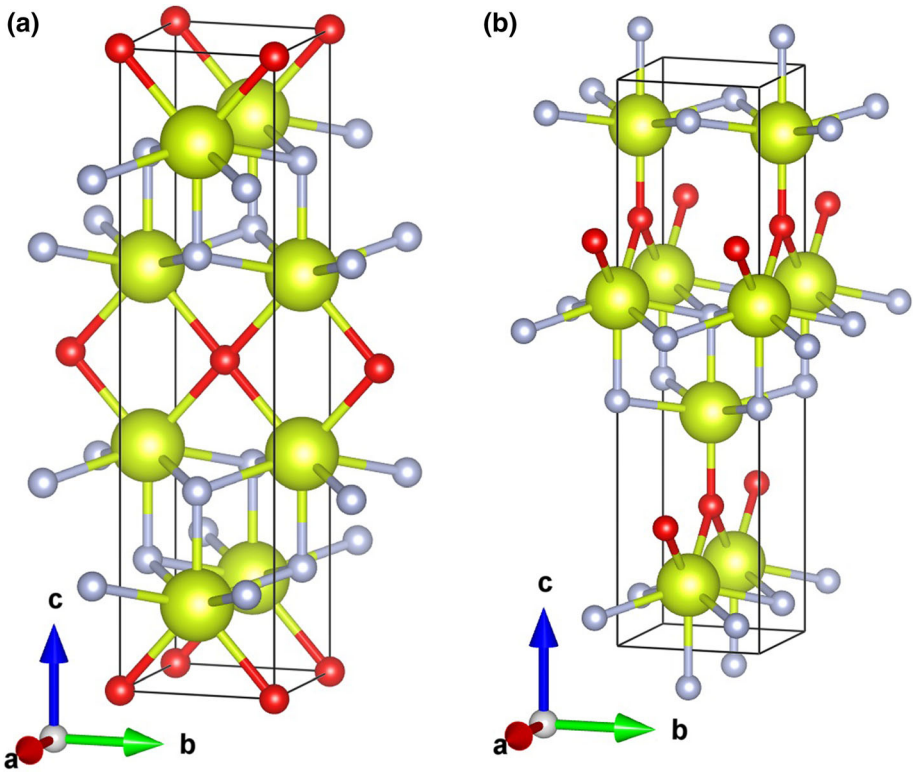

Fig. 1 Visualization of important but energetically unfavorable structure candidates: (a) Ce_2ON_2-*nf*-1 modification in space group *Immm* (no. 71); (b) Ce_2ON_2-*nf*-2 modification in space group *Amm*2 (no. 38). Yellow, red and grey spheres denote Ce, O and N atoms, respectively

the mean distance is 2.38 Å, which together with the seven-fold coordination of the Ce-atoms is expected and suggests a good structure candidate, in principle—at least on the level of the crystallographic analysis.

Another very interesting structure candidate among those with $Z = 1$ (Table 1) appears in the space group *Amm*2 (no. 38); this structure is shown in Fig. 1(b). Again, after ab initio refinement, this structure becomes energetically unfavorable, and thus it is denoted as Ce_2ON_2-*nf*-2 modification. Here, we note that structure candidates with space group *Cm* (no. 8) converted to this Ce_2ON_2-*nf*-2 modification, confirming it as a large local minima basin on the energy landscape. In this structure, we find two different Ce coordination polyhedra: a sevenfold coordinated Ce-atom (with distances 2 × 2.28 Å—O, 4 × 2.44 Å—N, 1 × 2.36 Å—N) and a six-fold coordinated Ce-atom (with distances 1 × 2.17 Å—O, 4 × 2.41 Å—N, 1 × 2.22 Å—N), respectively.

On the energy landscape of Ce_2ON_2 with $Z = 1$, two additional structure candidates appear to be of interest, although they are ranked as energetically unfavorable after the local optimization with DFT. The first is an orthorhombic candidate showing space group *Pmm*2 (no. 25), which is observed as a high-pressure modification on empirical potential level. It has been denoted the Ce_2ON_2-*nf*-3 structure, with a 7-fold coordination of cerium as shown in Fig. 2(a). Finally, there is a structure candidate with a tetragonal symmetry, which is not often found on the energy landscape but possesses the highest symmetry of all candidates. It has been named the Ce_2ON_2-*nf*-4 modification, appearing in space group *I*4/*mmm* (no. 139) with 6-fold coordination of Ce by O- and N-atoms (Fig. 2b).

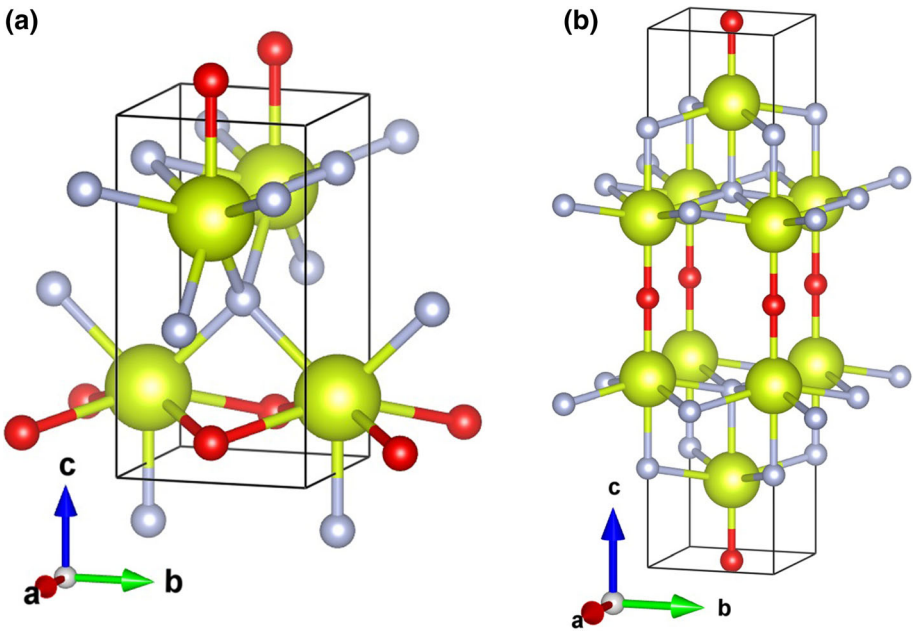

Fig. 2 Visualization of interesting but energetically unfavorable structure candidates: (a) Ce_2ON_2-*nf*-3 modification in space group *Pmm*2 (no. 25); (b) Ce_2ON_2-*nf*-4 modification in space group *I*4/*mmm* (no. 139). Notation as in Fig. 1

Analogous statistical and crystallographic analysis of the enthalpy landscapes with 2 and 3 formula units at pressures up to 160 GPa are presented in the Supporting Information (Tables S1 and S2). We note that with the increase of the number of formula units we observe more local minima associated with defect structures or several different coordination polyhedra of Ce-atoms by O- and N-atoms. This is not unexpected since once the composition of the chemical system exceeds two types of atoms, the number of local minima that correspond to structures containing "defects" increases, and thus most of the structure candidates show *P*1 (no. 1) symmetry. However, we would like to highlight the energetically most favorable structure candidates from the $Z = 2$, 3 energy landscapes. For example, the global minimum observed for $Z = 1$ is again found as the lowest energy structure for $Z = 2$, showing space group *C*2/*m* (no. 12) (Table S1). As for $Z = 1$, after further structure optimization on ab initio level, these candidates converted to the α-Ce_2ON_2 modification with space group *P*-3*m*1 (no. 164). In addition, two candidates denoted the β-Ce_2ON_2 modification with space group $Cmc2_1$ (no. 36) and the ε-Ce_2ON_2 modification, showing space group $P4_22_12$ (no. 94), respectively, have been found on these energy landscapes as energetically favorable structures (see Supporting Information). More details regarding these structure candidates will be presented in section 3.3.

3.2 Data Mining Based Searches Using ICSD

The data-mining search employed the ICSD database,[34] which contains 216,302 inorganic structures, out of which more than 80% have already been assigned to specific structure types (up to now, 9397 structure types are listed in the ICSD).[35] The first step of selection and pre-processing has been performed in order to reduce the number of structure candidates to a more manageable size. The first goal was to find the minimum number of unique structure candidates (prototypes) in the ternary A_2BC_2 system. In our first run through the database, we have selected from the complete ICSD database (> 200,000 structures), the 75,056 structures which belong to the ternary systems. In the next step, we have further reduced the number of structure candidates to 4754 using chemical elements search and by keeping only structures having the A_2BC_2 formula. Finally, we have further filtered the results by introducing the prototype criterion, where we assign a unique prototype to all structures with the same symmetry group, which can be mapped into each other by an overall rescaling where the different atom types in the A_2BC_2 formulae are matched appropriately.

Using the prototype criterion to eliminate quasi-duplicate structures reduced the number of structures by about two orders of magnitude, yielding 29 unique structure candidates: $AlCo_2Pr_2$, $AlFe_2B_2$, $BaCu_2S_2$, $BaZn_2P_2$, Be_2CaGe_2, $CaRh_2B_2$, Ce_2BiO_2, Ce_2Ni_2Sn, $CeAl_2Ga_2$, $CoCl_2(H_2O)_2$, CoW_2B_2, $CoZr_2Si_2$, Cu_2BaO_2, Dy_2OS_2, Ge_2LaPt_2, K_2GaP_2, K_2MnS_2, K_2PdP_2, K_2PtS_2, LaB_2C_2, Li_2PdO_2, Na_2HgO_2, Na_2PtS_2, Sc_2O_2S, Si_2N_2O, Th_2TeN_2, Yb_2S_2O, $Zn(CN)_2$, Zr_2NiAs_2. Note that these prototypical structures can be used in any future study involving A_2BC_2 systems (for more details and references, see the Supporting Information).

After local optimization on ab initio level using DFT-LDA, most of the structure candidates obtained from data mining have become energetically unfavorable compared to those candidates obtained via the global optimization. Space group, unit cell parameters (Å) and atomic positions for the unfavorable Ce_2ON_2 modifications after LDA optimization are given in the Table S3.

However, there were two notable exceptions: when we start the ab initio optimization from the $AlCo_2Pr_2$[51] structure type, we obtain the lowest energy minimum among the data-mined candidates, which also corresponds to the α-Ce_2ON_2 modification determined via global optimization. A second energetically favorable structure, denoted the γ-Ce_2ON_2 modification, was obtained from minimizing the Dy_2OS_2[52] prototype. In both instances, the generic structure of the starting prototype candidate was only slightly changed during the local ab initio optimization.

Furthermore, among the modifications with high energy, two interesting hexagonal structure candidates, which we call Ce_2ON_2-*nf*-5 and Ce_2ON_2-*nf*-7, have been identified from among the data-mined candidates, and subsequently optimized. Although both structures appear in the same space group ($P6_3/mmc$, no. 194), the Ce_2ON_2-*nf*-5 modification shows the Sc_2O_2S structure type,[53] while the Ce_2ON_2-*nf*-7 modification shows the Zr_2NiAs_2 structure type,[54] respectively. In addition, Ce_2ON_2-*nf*-7 is higher in energy than Ce_2ON_2-*nf*-5, or other feasible candidates obtained from data mining (Table 2). Finally, a tetragonal modification has been found using data mining and denoted as Ce_2ON_2-*nf*-6. This structure appears in the $P4/nmm$ space group (no. 129) with Be_2CaGe_2 structure type;[55] however it is unlikely to be synthesized because of its very high energy. The five most relevant structure candidates from data mining based searches, with their energies after local ab initio relaxations, are presented in Table 2.

3.3 E(V)-Curves on LDA Level

Figure 3 presents the energy versus volume curves on ab initio level using the LDA functional of the five most relevant structure candidates in the Ce_2ON_2 system, while their structural informations are listed in Table 3. The α-modification of the Ce_2ON_2 compound exhibits trigonal space group $P\text{-}3m1$ (no.164) with an $AlCo_2Pr_2$-like structure after the local optimization. Cerium is 7-fold coordinated (atom–atom distances: 3 × 2.25 Å—N; 1 × 2.27 Å—N; and 3 × 2.57 Å—O), with a mean distance of about 2.39 Å, as expected from the typical ionic radii of the Ce-, O- and N-atoms (see Fig. 4a and Table 3).[56] Here, we note several points: (a) the predicted α-modification has been found as a distorted version with lower symmetry on the empirical potential energy landscape using global optimization; (b) using data mining based searches, the α-modification has been found starting from the $AlCo_2Pr_2$[51] prototype, and the local optimization resulted in a closely related structure type ($AlCo_2Pr_2$-like); (c) according to the E(V) curves, the α-Ce_2ON_2 modification is the unique equilibrium structure type and global energy minimum among the single phase compounds with composition Ce_2ON_2—at least up to moderately elevated pressures as shown in Fig. 3 -; (d) the α-modification was found via both global optimization and data mining as the lowest energy structure in both sets of structure candidates, and exhibited the lowest energy for both empirical potential and ab initio calculations.

The β-Ce_2ON_2 structure candidate exhibits the space group $Cmc2_1$ (no. 36) and has also been found after the global search. Here, the Ce-atoms are coordinated by 7

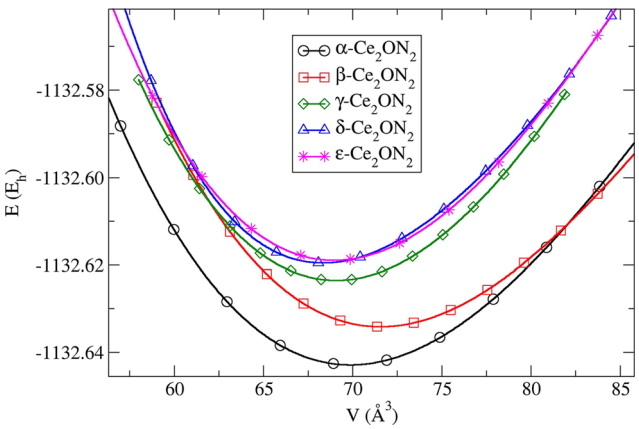

Fig. 3 Energy vs. volume, $E(V)$, curves for the five most relevant structure candidates of Ce_2ON_2 calculated using the LDA functional. Note that we are plotting the potential energy as function of volume, not a free energy or enthalpy, i.e. neither temperature nor pressure are involved. Energies per formula unit are given in hartree (E_h)

Table 2 The most relevant structure candidates from data mining based searches, after local ab initio relaxations

Modification	Structure type	Space group (no.)	Total energy, eV/atom	Total energy, kJ/mol-atoms
α-Ce_2ON_2	$AlCo_2Pr_2$-like	164	− 6164.1571	− 594,748.70
γ-Ce_2ON_2	Dy_2OS_2	62	− 6164.0520	− 594,738.56
Ce_2ON_2-*nf*-5	Sc_2O_2S	194	− 6164.0031	− 594,733.84
Ce_2ON_2-*nf*-6	Be_2CaGe_2	129	− 6164.6085	− 594,695.77
Ce_2ON_2-*nf*-7	Zr_2NiAs_2	194	− 6163.3723	− 594,672.98

Table 3 Modification, space group, unit cell parameters (Å), atomic positions and total energy values in eV/atom (kJ/mol-atoms) for the most relevant Ce_2ON_2 modifications after LDA optimization

Modification and space group	LDA		Total energy, eV/atom, kJ/mol-atoms	Difference, eV/atom, kJ/mol-atoms, %
	Cell paramaters, Å and atomic positions	Bond distances, Å		
α-Ce_2ON_2	a = 3.77, c = 5.57	Ce-N 3 × 2.2536	− 6164.1571	–
P-3*m*1 (164)	Ce (2/3 1/3 0.7440) 2d	Ce-N 1 × 2.2752	− 594,748.70	
	O (0 0 1/2) 1b	Ce-O 3 × 2.5674		
	N (1/3 2/3 0.8476) 2d	Mean: 2.3912 (VII)		
β-Ce_2ON_2	a = 3.57, b = 13.81, c = 5.76	Ce-N 2 × 2.4300	− 6164.1130	− 0.0441
Cmc2_1 (36)	Ce (0 0.8128 0.9167) 4a	Ce-N 2 × 2.4334	− 594,744.44	− 4.25
	Ce (0 0.5481 0.9774) 4a	Ce-N 1 × 2.1840		0.0007%
	O (0 0.6447 0.6613) 4a	Ce-O 1 × 2.2575		
	N (0 0.3146 0.6656) 4a	Ce-O 1 × 2.8666		
	N (0 0.0304 0.2616) 4a	Mean: 2.4336 (VII)		
γ-Ce_2ON_2	a = 13.22, b = 3.47, c = 5.93	Ce-N 2 × 2.3301	− 6164.0520	− 0.1051
Pnma (62)	Ce (0.4432 1/4 0.7527) 4c	Ce-N 2 × 2.5270	− 594,738.56	− 10.13
	Ce (0.3054 1/4 0.2655) 4c	Ce-N 1 × 2.2089		0.0017%
	O (0.4689 1/4 0.3534) 4c	Ce-N 1 × 2.8719		
	N (0.1175 1/4 0.5079) 4c	Ce-O 1 × 2.2236		
	N (0.1779 1/4 0.0250) 4c	Mean: 2.4312 (VII)		
δ-Ce_2ON_2	a = 3.32, c = 6.23	Ce-N 4 × 2.4154	− 6164.0308	− 0.1263
P-4*m*2 (115)	Ce (0 1/2 0.7728) 2d	Ce-N 1 × 2.2584	− 594,736.51	− 12.18
	O (0 0 1/2) 1d	Ce-O 2 × 2.3743		0.002%
	N (1/2 0 0.8645) 2 g	Mean: 2.3812 (VII)		
ε-Ce_2ON_2	a = 3.32, c = 12.43	Ce-N 4 × 2.4160	− 6164.0341	− 0.1203
P4_2/*nmc* (137)	Ce (1/4 1/4 0.1136) 4d	Ce-N 1 × 2.2573	− 594,736.83	− 11.87
	O (3/4 1/4/1/4) 2b	Ce-O 2 × 2.3734		0.002%
	N (3/4 3/4 0.5680) 4d	Mean: 2.3812 (VII)		

Analogous data for the most relevant but energetically unfavorable modifications is given in table S3 of the Supporting Information

anions, similar as in the α-modification; however, cerium is surrounded with 5 nitrogen and 2 oxygen atoms (instead of 4 + 3 as in the α-modification). Full structural data is presented in Table 3 and the structure is depicted in Fig. 4(b). The β-modification is the energetically favorable stable structure in the effective negative pressure region where low-density structures are preferred, in principle (c.f. the region with large volumes, V > 80 $Å^3$ in Fig. 3). This could indicate a possible synthesis route via, e.g., crystallization from an amorphous phase deposited from the gas phase, such as was recently used in the synthesis of a new gallium modification (β'-gallium).[57]

The γ-Ce_2ON_2 modification possesses the *Pnma* space group (no. 62), following the Dy_2OS_2[52] prototype. This structure candidate has been found only after data mining based searches, and according to the total energy ranking it might be capable of existence perhaps as a metastable modification (Fig. 3 and Table 3). Structurally, the γ-modification is particularly interesting since cerium is found with two different coordination polyhedra. In the first, the Ce-atoms are seven-fold coordinated, with 1 oxygen and 6 nitrogen atoms, while in the second, the Ce-atoms are eight-fold coordinated, with 3 oxygen and 5 nitrogen atoms (see Fig. 4c).

Next, the δ-Ce_2ON_2 modification has been found as the preferred modification at high pressures during global searches with empirical potential, where it exhibits the space group *P*4*m*2 (no. 115) with cerium coordinated by

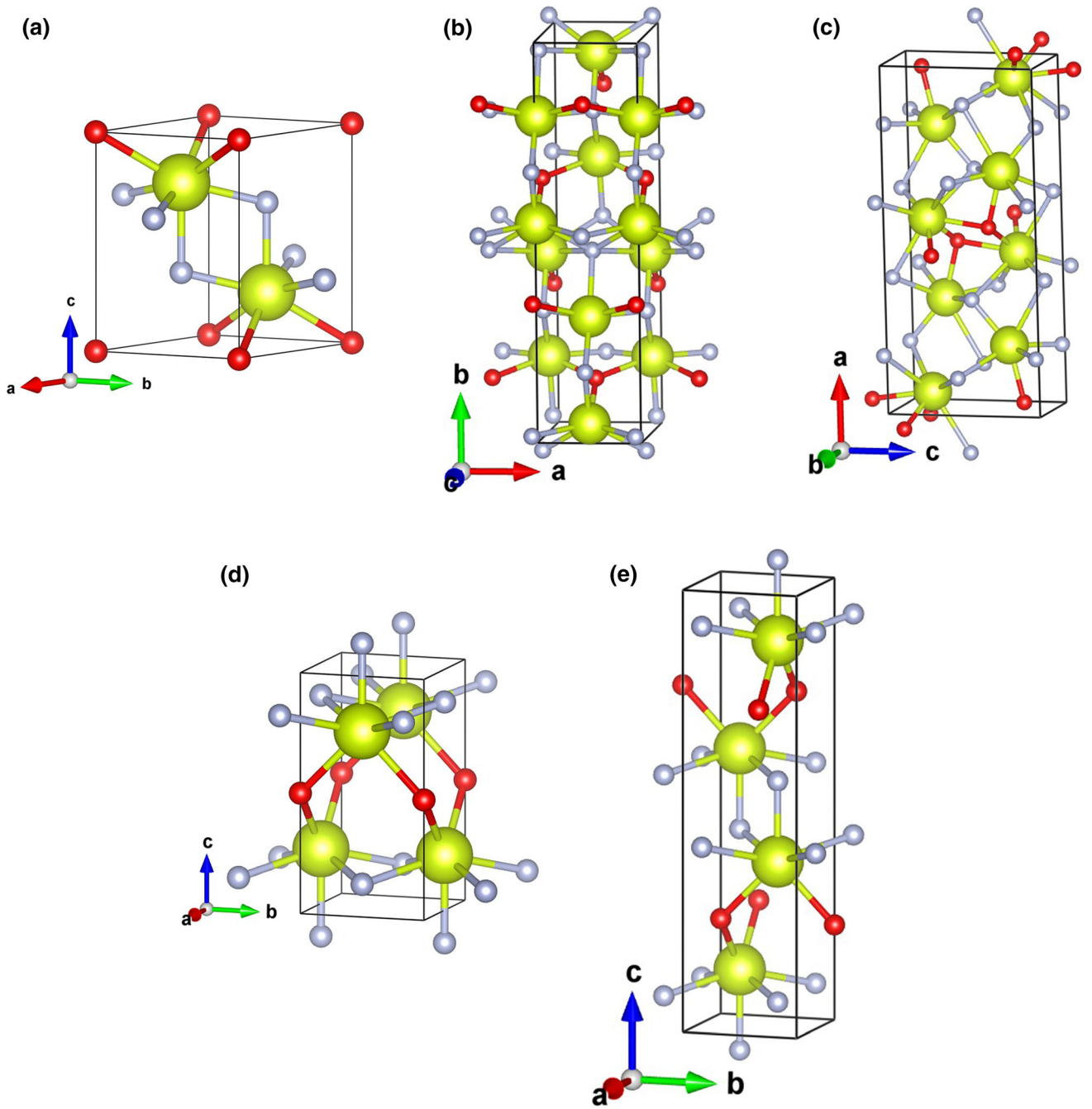

Fig. 4 The best five Ce_2ON_2 candidates found during the global energy landscape search and via the data mining: (a) α-Ce_2ON_2 (S.G. 164); (b) β-Ce_2ON_2 (S.G. 36); (c) γ-Ce_2ON_2 (S.G. 62); (d) δ-Ce_2ON_2 (S. G. 115) and (e) ε-Ce_2ON_2 (S. G. 137). Notation as in Fig. 1

five nitrogen and two oxygen atoms (Fig. 4d). After DFT optimization, the structure appears to be at best a metastable phase, which would probably need elevated pressures and temperatures during synthesis because of its high energy (Fig. 3, Tables 1 and 3). However, for pressures relevant to the E(V) curves in Fig. 3, the α-Ce_2ON_2 modification should still have the highest relative thermodynamical stability among the various modifications at $T = 0$ K. In this context, we note that in Fig. 3, we have not included the E(V) curves of those other candidates that might perhaps be competitive at extremely high pressures but are clearly irrelevant at standard pressure, such as Ce_2ON_2-nf-6 and Ce_2ON_2-nf-7: they exhibit eight- and nine-fold coordinated cerium ions, respectively, as one would expect for high-pressure structures, but have very unfavorable total energy values (Ce_2ON_2-nf-6: − 1132.5417 Hartrees and Ce_2ON_2-nf-7: − 1132.4982 Hartrees).

Finally, the ε-Ce_2ON_2 modification, showing space group $P4_22_12$ (no. 94), has been found on the enthalpy landscape as an energetically favorable candidate at extremely high pressures of 160 GPa. After *ab intio* local optimization at standard pressure, the ε-modification has converted to a possibly metastable modification in the space group $P4_2/nmc$ (no. 137), with cerium 7-fold coordinated (Fig. 4e), although its energy is quite high, of course, compared to the other structure candidates.

We note that the δ- and ε-modifications are closely related: they are energetically close, both indicate the need for high-pressure and high-temperature synthesis conditions if they are accessible at all, and both appear in tetragonal symmetry (Fig. 3, Tables 1 and 3). Furthermore, they are structurally related having the same coordination polyhedra, where the ε-modification creates another layer by tilting the same basic polyhedra, thus becoming a polytype of the δ-modification (Fig. 4d and e). Finally, it is interesting to note that in each of the five relevant structure candidates, the cerium cations are seven-fold coordinated by the anions, where the only difference is the shape of the coordination polyhedra and the way they are connected.

4 Discussion

Of course, it would be of interest to know whether α-Ce_2ON_2 would be stable against decomposition into e.g. Ce(+IV)O_2 and Ce(+IV)$_3N_4$, via 2 Ce_2ON_2 ⇌ CeO_2 + Ce_3N_4. While Ce(+IV)O_2 is well-known, no compound Ce(+IV)$_3N_4$ is known to exist, and thus, for a rough estimate of the likelihood of a decomposition, we have computed the ab initio energy of a hypothetical Ce(+IV)$_3N_4$ modification in a typical A_3N_4 structure type, Si_3N_4 (also known as the Nb_3Te_4 structure type). We find that α-Ce_2ON_2 is relatively stable against such a hypothetical decomposition, since the energy of 2 formula units of α-Ce_2ON_2 is lower than the energy of the sum of one formula unit of CeO_2 and Ce_3N_4, -61,641.571 eV < − 16,986.2775 eV + (− 44,653.2461 eV), i.e. the energy difference per atom is ($2E_{fu}(Ce_2ON_2)$ − ($E_{fu}(CeO_2)$- + $E_{fu}(Ce_3N_4)$))/10 = − 0.2047 eV/atom (− 19.74 kJ/mol-atoms) is negative. Clearly, this is not a final answer, since a global energy landscape study for Ce_3N_4 would be required to obtain the lowest energy modification of Ce_3N_4—the Si_3N_4-type is an educated guess -; furthermore, one would need to take the possibility of a decomposition into CeN, via e.g. α-Ce_2ON_2 ⇌ 1/2O_2 + 2CeN, or a multitude of other decomposition paths into various cerium oxynitrides (plus oxygen and/or nitrogen), into account, in principle. However, such a study of the competition between cerium oxynitride compounds containing both Ce(+III) and Ce(+IV), including mixed valence compounds, is beyond the purview of the current investigation.

Nevertheless, as a first estimate, we have computed the relative stability of α-Ce_2ON_2 against decomposition into the solid elements, 2 Ce(solid) + O(solid) + 2 N(solid), and against decomposition of two α-Ce_2ON_2 into CeO_2- + 3CeN + N(solid). Of course, our calculations do not account for temperature, and thus these decompositions only refer to T = 0 K. Table 4 shows the energies for the compounds and elements involved in these estimates, computed on DFT level with CRYSTAL17, using the same basis sets for consistency.

First, we note that CeO_2 is stable against decomposition into Ce_2O_3 and O_{solid} by comparing the energies of 2 formula units of CeO_2 with the sum of one formula unit of Ce_2O_3 and O_{solid}: 2 E_{fu} (CeO_2) = − 33,972.5550 eV < $E_{fu}(Ce_2O_3)$ + $E_{fu}(O_{solid})$ = − 31,935.2407 eV + (− 2030.9471 eV) = − 33,966.1878 eV, i.e. the energy difference per atom is (2 $E_{fu}(CeO_2)$ − ($E_{fu}(Ce_2O_3)$ + E_{fu}(O)))/6 = − 1.0612 eV/atom (− 102.39 kJ/mol-atoms), and thus at T = 0 K, CeO_2 is relatively stable against the above decomposition at T = 0 K. Similarly, we consider the hypothetical Ce_3N_4 compound and its decomposition into CeN and N_{solid}: $E_{fu}(Ce_3N_4)$ = − 44,653.2461 eV < 3 E_{fu}(CeN) + $E_{fu}(N_{solid})$ = − 44,653.2139 eV, i.e. the energy difference per atom is ($E_{fu}(Ce_3N_4)$ − (3 E_{fu}(CeN) + $E_{fu}(N_{solid})$))/7 = − 0.0046 eV/atom (− 0.44 kJ/mol-atoms), and thus, we conclude that at T = 0 K, the hypothetical Ce_3N_4 should be marginally relatively stable against decomposition into CeN and N_{solid}. Thus, it appears that the oxidation state Ce(+IV) is preferred to Ce(+III), at least within the context of the LCAO-basis DFT ab initio calculations we have employed, in agreement with the common occurence of CeO_2 in nature.

Now, for the decomposition of α-Ce_2ON_2 into the elements (all in the solid state at T = 0 K!), we find E_{fu}(α-Ce_2ON_2) = − 30,820.7855 eV < 2 E_{fu}(Ce) + $E_{fu}(O_{solid})$- + 2 $E_{fu}(N_{solid})$ = − 7563.4721 eV, i.e. the energy difference per atom is (E_{fu}(α-Ce_2ON_2) − (2 E_{fu}(Ce) + $E_{fu}(O_{solid})$ + 2 $E_{fu}(N_{solid})$))/5 = − 4651.4627 eV/atom (− 448,796.38 kJ/mol-atoms). Thus α-Ce_2ON_2 is relatively stable against decomposition into the elements, at least close to T = 0 K. Similarly, for a decomposition into CeN, CeO_2 and solid nitrogen, we find 2 E_{fu}(α-Ce_2ON_2) = -61,641.5710 eV < $E_{fu}(CeO_2)$ + 3 E_{fu}(CeN) + $E_{fu}(N_{solid})$- = − 61,639.4914 eV, i.e. the energy difference per atom is (2 E_{fu}(α-Ce_2ON_2) − (E_{fu} (CeO_2) + 3 E_{fu}(CeN) + E_{fu}(-N_{solid})))/10 = − 0.2080 eV/atom (-20.07 kJ/mol-atoms), which again demonstrates the hypothetical compound's relative stability against the outlined decomposition. From this we would conclude that our estimate suggests that α-Ce_2ON_2 should be at least be metastable thermodynamically at non-zero temperatures even though it might lose

Table 4 Energies of the compounds and elements, computed using DFT

Compound/Element	E_{fu}	E_{at}
Ce_2O_3	− 31,935.2420 eV/f.u.	− 6387.0484 eV/atom
	− 3,081,271.82 kJ/mol-f.u.	− 616,254.36 kJ/mol-atoms
O(solid)(a)	− 2030.9471 eV/f.u.	− 2030.9471 eV/atom
	− 195,955.93 kJ/mol-f.u.	− 195,955.93 kJ/mol-atoms
CeO_2	− 16,986.2775 eV/f.u.	− 5662.0925 eV/atom
	− 1,638,920.98 kJ/mol-f.u.	− 546,306.99 kJ/mol-atoms
Ce_3N_4	− 44,653.2464 eV/f.u.	− 6379.0352 eV/atom
	− 4,308,368.48 kJ/mol-f.u.	− 615,481.21 kJ/mol-atoms
CeN	− 14,392.4628 eV/f.u.	− 7196.2314 eV/atom
	− 1,388,656.77 kJ/mol-f.u.	− 694.328.39 kJ/mol-atoms
N(solid)(a)	− 1475.8258 eV/f.u.	− 1475.8258 eV/atom
	− 142,395.05 kJ/mol-f.u.	− 142,395.05 kJ/mol-atoms
Ce	− 1290.4367 eV/f.u.	− 1290.4367 eV/atom
	− 124,507.78 kJ/mol-f.u.	− 124,507.78 kJ/mol-atoms

Both the energy per atom (E_{at}) and the energy per formula unit (E_{fu}) are given, in eV and kJ/mol. (a) Solid oxygen has been calculated in the space group R-3m, and solid nitrogen in the space group $P2_13$

nitrogen and/or oxygen at temperatures, where these elements are gaseous. Figure S1 in the supplementary material shows a rudimentary $T = 0$ K (triangular) composition phase diagram, with the computed data points (hypothetical α-Ce_2ON_2, hypothetical Ce_3N_4, CeN, CeO_2, solid nitrogen, solid oxygen, and metallic Ce).

Clearly, at standard conditions, both oxygen and nitrogen are gaseous, and thus there will be a large contribution to the free energy from the entropy, similar to the one for an ideal gas. This will influence all the decompositions given above. However, the focus of this study has been the prediction of feasible structure candidates for the compound Ce_2ON_2, as a first step towards the exploration of the Ce-O-N system, and the effects of temperature and thus the presence of oxygen and nitrogen in the gaseous phase on the stability of this compound goes beyond the purview of this investigation. Thus, we also do not make assertions about the absolute thermodynamic stability of these hypothetical modifications of a Ce_2ON_2 compound, but only refer to their relative thermodynamic stability.

5 Conclusions

In this study, we have explored the energy landscape of the hypothetical ionic cerium oxynitride Ce_2ON_2 ceramic, and predicted several feasible modifications for this compound for the first time. The discovery of new theoretical modifications in the predicted system has been achieved using global optimization and data mining, where the energy landscape has been explored for various pressures and different numbers of formula units in the simulation cell. The global optimization has been performed with empirical potentials, with subsequent local minimization on the ab initio level. From more than 14,000 structure candidates obtained after global optimization with simulated annealing, plus the 29 potential structure candidates found via data mining and prototyping, we have obtained five highly plausible low-energy modifications that might be realized as (meta)stable modifications, plus seven crystallographically and chemically interesting but energetically unfavorable structures.

Among the hypothetical Ce_2ON_2 solid modifications, the α-Ce_2ON_2 modification, with an $AlCo_2Pr_2$-like structure, is predicted to be the one with the highest relative thermodynamic stability, at least at low temperatures, while at effective negative pressures, the β-Ce_2ON_2 modification should exhibit the highest relative thermodynamic stability, and be synthetically accessible. Two predicted orthorhombic modifications might be metastable, the already mentioned β-modification and the γ-modification. Finally, high temperatures combined with high pressures might favor the existence of the δ- or the ε-modification as metastable structures. Clearly, this is only a first step towards the full phase diagram in the Ce-O-N system, where one would include temperature and also investigate many more ternary, and even binary compositions. Nevertheless, this work provides a first glimpse of the potential structural richness of the Ce-O-N system.

Acknowledgments Open Access funding provided by Projekt DEAL. The authors are grateful to prof. R. Dovesi, K. Doll, and Crystal Solutions for software support with CRYSTAL code. Also this project was financially supported by the Ministry of Education, Science and Technological Development of Serbia (Project Number: III45012).

References

1. A.B. Jorge, J. Fraxedas, A. Cantarero, A.J. Williams, J. Rodgers, J.P. Attfield, and A. Fuertes, Nitrogen Doping of Ceria, *Chem. Mater.*, 2008, **20**, p 1682-1684
2. M. Weishaupt and J. Strähle, Darstellung der Oxidnitride VON, NbON und TaON. Die Kristallstruktur von NbON und TaON, *Z. Anorg. Allg. Chem.*, 1977, **429**, p 261-269
3. J.-S. Lee, M. Lerch, and J. Maier, Nitrogen-Doped Zirconia: A Comparison with Cation Stabilized Zirconia, *J. Solid State Chem.*, 2006, **179**, p 270-277
4. M. Das, S. Patil, N. Bhargava, J.-F. Kang, L.M. Riedel, S. Seal, and J.J. Hickman, Auto-Catalytic Ceria Nanoparticles Offer Neuroprotection to Adult Rat Spinal Cord Neurons, *Biomaterials*, 2007, **28**, p 1918-1925
5. T. Masui, M. Yamamoto, T. Sakata, H. Mori, and G.-Y. Adachi, Synthesis of BN-Coated CeO_2 Fine Powder as a New UV Blocking Material, *J. Mater. Chem.*, 2000, **10**, p 353-357
6. S. Park, J.M. Vohs, and R.J. Gorte, Direct Oxidation of Hydrocarbons in a Solid-Oxide Fuel Cell, *Nature*, 2000, **404**, p 265-267
7. A. Corma, P. Atienzar, H. García, and J.-Y. Chane-Ching, Hierarchically Mesostructured Doped CeO_2 with Potential for Solar-Cell Use, *Nat. Mater.*, 2004, **3**, p 394-397
8. B. Matovic, D. Nikolic, N. Labus, S. Ilic, V. Maksimovic, J. Lukovic, and D. Bucevac, Preparation and Properties of Porous, Biomorphic, Ceria Ceramics for Immobilization of Sr Isotopes, *Ceram. Int.*, 2013, **39**, p 9645-9649
9. D. Bucevac, A. Radojkovic, M. Miljkovic, B. Babic, and B. Matovic, Effect of Preparation Route on the Microstructure and Electrical Conductivity of Co-doped ceria, *Ceram. Int.*, 2013, **39**, p 3603-3611
10. V. Prabhakaran and V. Ramani, Structurally-Tuned Nitrogen-Doped Cerium Oxide Exhibits Exceptional Regenerative Free Radical Scavenging Activity in Polymer Electrolytes, *J. Electrochem. Soc.*, 2013, **161**, p F1-F9
11. Y.-C. Zhang, Y.-K. Liu, L. Zhang, E. Xiu-tian-feng, L. Pan, X. Zhang, A. Fazal e, D.-R. Zou, S.-H. Liu, and J.-J. Zou, DFT study on water oxidation on nitrogen-doped ceria oxide, *Appl. Surf. Sci.*, 2018, **452**, p 423-428
12. C. Mao, Y. Zhao, X. Qiu, J. Zhu, and C. Burda, Synthesis, Characterization and Computational Study of Nitrogen-Doped CeO_2 Nanoparticles with Visible-Light Activity, *Phys. Chem. Chem. Phys.*, 2008, **10**, p 5633-5638
13. H. Shi, T. Hussain, R. Ahuja, T.W. Kang, and W. Luo, Role of Vacancies, Light Elements and Rare-Earth Metals Doping in CeO_2, *Sci. Rep.*, 2016, **6**, p 31345
14. B. Matović, J. Dukić, B. Babić, D. Bučevac, Z. Dohčević-Mitrović, M. Radović, and S. Bošković, Synthesis, Calcination and Characterization of Nanosized Ceria Powders by Self-propagating Room Temperature Method, *Ceram. Int.*, 2013, **39**, p 5007-5012
15. S. Dmitrović, M.G. Nikolić, B. Jelenković, M. Prekajski, M. Rabasović, A. Zarubica, G. Branković, and B. Matović, Photoluminescent Properties of Spider Silk Coated with Eu-Doped Nanoceria, *J. Nanopart. Res.*, 2017, **19**, p 47
16. D. Mićović, M.C. Pagnacco, P. Banković, J. Maletaškić, B. Matović, V.R. Djokić, and M. Stojmenović, The Influence of Short Thermal Treatment on Structure, Morphology and Optical Properties of Er and Pr Doped Ceria Pigments: Comparative Study, *Process. Appl. Ceram.*, 2019, **13**, p 310-321
17. G.A. Landrum, R. Dronskowski, R. Niewa, and F.J. DiSalvo, Electronic Structure and Bonding in Cerium (Nitride) Compounds: Trivalent Versus Tetravalent Cerium, *Chem. A Eur. J.*, 1999, **5**, p 515-522
18. A. Delin, P.M. Oppeneer, M.S.S. Brooks, T. Kraft, J.M. Wills, B. Johansson, and O. Eriksson, Optical Evidence of 4f-Band Formation in CeN, *Phys. Rev. B*, 1997, **55**, p R10173-R10176
19. G.I. Panov and A.S. Kharitonov, Catalytic properties of nitrides in ammonia synthesis, *React. Kinet. Catal. Lett.*, 1985, **29**, p 267-274
20. C. Heinrichs, Synthesis and Characterization of Anhydrous Rare Earth Metal Nitrates, Acetates and Oxyacetates, Koeln University, Verlag Dr. Hut (2013)
21. A. Dastgheib, M. Mohammadzadeh Attar, and A. Zarebidaki, Evaluation of Corrosion Inhibition of Mild Steel in 3.5 wt% NaCl Solution by Cerium Nitrate. Metals and Materials International (2019)
22. M. WoŁcyrz and L. Kepinski, Rietveld Refinement of the Structure of CeOCI, Formed in Pd/CeO_2 Catalyst: Notes on the Existence of a Stabilized Tetragonal Phase of La_2O_3 in La-Pd-O System, *J. Solid State Chem.*, 1992, **99**, p 409-413
23. M. Coduri, M. Scavini, M. Allieta, M. Brunelli, and C. Ferrero, Defect Structure of Y-Doped Ceria on Different Length Scales, *Chem. Mater.*, 2013, **25**, p 4278-4289
24. E. Mamontov, T. Egami, R. Brezny, M. Koranne, and S. Tyagi, Lattice Defects and Oxygen Storage Capacity of Nanocrystalline Ceria and Ceria-Zirconia, *J. Phys. Chem. B*, 2000, **104**, p 11110-11116
25. N.V. Skorodumova, R. Ahuja, S.I. Simak, I.A. Abrikosov, B. Johansson, and B.I. Lundqvist, Electronic, Bonding, and Optical Properties of CeO_2 and Ce_2O_3 from First Principles, *Phys. Rev. B*, 2001, **64**, p 115108
26. G.L. Olcese, Interconfiguration Fluctuation of Cerium in CeN as a Function of Temperature and Pressure, *J. Phys. F Met. Phys.*, 1979, **9**, p 569-578
27. M. Čebela, D. Zagorac, K. Batalović, J. Radaković, B. Stojadinović, V. Spasojević, and R. Hercigonja, $BiFeO_3$ Perovskites: A Multidisciplinary Approach to Multiferroics, *Ceram. Int.*, 2017, **43**, p 1256-1264
28. J. Zagorac, D. Zagorac, M. Rosić, J.C. Schön, and B. Matović, Structure Prediction of Aluminum Nitride Combining Data Mining and Quantum Mechanics, *CrystEngComm*, 2017, **19**, p 5259-5268
29. D. Zagorac, J.C. Schön, M. Rosić, J. Zagorac, D. Jordanov, J. Luković, and B. Matović, Theoretical and Experimental Study of Structural Phases in $CoMoO_4$, *Cryst. Res. Technol.*, 2017, **52**, p 1700069
30. S. Kirkpatrick, C.D. Gelatt, and M.P. Vecchi, Optimization by Simulated Annealing, *Science*, 1983, **220**, p 671-680
31. J.C. Schön, Nanomaterials—What Energy Landscapes Can Tell Us, *Process. Appl. Ceram.*, 2015, **9**, p 157-168
32. J.C. Schön, G42+ Manual, Stuttgart, 2015; website: https://www.chemie.uni-bonn.de/ac/schoen/forschung/g42-manual.

33. J.C. Schön and M. Jansen, Determination of Candidate Structures for Simple Ionic Compounds Through Cell Optimisation, *Comput. Mater. Sci.*, 1995, **4**, p 43-58
34. G. Bergerhoff and I.D. Brown, *Crystallographic Databases*, International Union of Crystallography, Chester, UK, 1987
35. D. Zagorac, H. Müller, S. Ruehl, J. Zagorac, and S. Rehme, Recent Developments in the Inorganic Crystal Structure Database: Theoretical Crystal Structure Data and Related Features, *J. Appl. Crystallogr.*, 2019, **52**, p 918-925
36. R. Allmann and R. Hinek, The Introduction of Structure Types into the Inorganic Crystal Structure Database ICSD, *Acta Crystallogr. Sect. A*, 2007, **63**, p 412-417
37. A.A. Sokol, C.R.A. Catlow, M. Miskufova, S.A. Shevlin, A.A. Al-Sunaidi, A. Walsh, and S.M. Woodley, On the Problem of Cluster Structure Diversity and the Value of Data Mining, *Phys. Chem. Chem. Phys.*, 2010, **12**, p 8438-8445
38. G. Ceder, D. Morgan, C. Fischer, K. Tibbetts, and S. Curtarolo, Data-Mining-Driven Quantum Mechanics for the Prediction of Structure, *MRS Bull.*, 2011, **31**, p 981-985
39. R. Dovesi, R. Orlando, B. Civalleri, C. Roetti, V. R. Saunders, and C. M. Zicovich-Wilson, CRYSTAL: A Computational Tool for the Ab Initio Study of the Electronic Properties of Crystals, *Z. Kristallogr. Cryst. Mater.*, 2005, **220**, p 571
40. K. Doll, R. Dovesi, and R. Orlando, Analytical Hartree-Fock Gradients with Respect to the Cell Parameter for Systems Periodic in Three Dimensions, *Theor. Chem. Acc.*, 2004, **112**, p 394-402
41. K. Doll, V.R. Saunders, and N.M. Harrison, Analytical Hartree-Fock Gradients for Periodic Systems, *Int. J. Quantum Chem.*, 2001, **82**, p 1-13
42. J. Graciani, A.M. Márquez, J.J. Plata, Y. Ortega, N.C. Hernández, A. Meyer, C.M. Zicovich-Wilson, and J.F. Sanz, Comparative Study on the Performance of Hybrid DFT Functionals in Highly Correlated Oxides: The Case of CeO_2 and Ce_2O_3, *J. Chem. Theory Comput.*, 2011, **7**, p 56-65
43. M.D. Towler, N.L. Allan, N.M. Harrison, V.R. Saunders, W.C. Mackrodt, and E. Aprà, Ab Initio Study Of MnO and NiO, *Phys. Rev. B*, 1994, **50**, p 5041-5054
44. D. Zagorac, J.C. Schön, J. Zagorac, and M. Jansen, Prediction of Structure Candidates for Zinc Oxide as a Function of Pressure and Investigation of Their Electronic Properties, *Phys. Rev. B*, 2014, **89**, p 075201
45. R. Dovesi, M. Causa', R. Orlando, C. Roetti, and V.R. Saunders, Ab Initio Approach to Molecular Crystals: A Periodic Hartree-Fock Study of Crystalline Urea, *J. Chem. Phys.*, 1990, **92**, p 7402-7411
46. D. Zagorac, J. Zagorac, M.B. Djukic, D. Jordanov, and B. Matović, Theoretical Study of AlN Mechanical Behaviour Under High Pressure Regime, *Theor. Appl. Fract. Mech.*, 2019, **103**, p 102289
47. R. Hundt, J.C. Schön, A. Hannemann, and M. Jansen, Determination of Symmetries and Idealized Cell Parameters for Simulated Structures, *J. Appl. Crystallogr.*, 1999, **32**, p 413-416
48. A. Hannemann, R. Hundt, J.C. Schön, and M. Jansen, A New Algorithm for Space-Group Determination, *J. Appl. Crystallogr.*, 1998, **31**, p 922-928
49. R. Hundt, *KPLOT, A Program for Plotting and Analyzing Crystal Structures*, Technicum Scientific Publishing, Stuttgart, 2016
50. K. Momma and F. Izumi, VESTA: A Three-Dimensional Visualization System for Electronic and Structural Analysis, *J. Appl. Crystallogr.*, 2008, **41**, p 653-658
51. M. Pani, D. Merlo, and M. Fornasini, Structure and Transport Properties of the R_2Co_2Al Compounds (R = Pr, Nd, Sm, Gd, Tb, Dy, Ho, Er, Tm, Y), *Z. Kristallogr.*, 2002, **217**, p 415-419
52. T. Schleid, Zwei Formen von Dy_2OS_2, *Zeitschrift für anorganische und allgemeine Chemie*, 1991, **602**, p 39-47
53. M. Julien-Pouzol, S. Jaulmes, M. Guittard, and P. Laruelle, Oxysulfure de Scandium Sc_2O_2S, *J. Solid State Chem.*, 1978, **26**, p 185-188
54. E.H. El Ghadraoui, J.Y. Pivan, R. Guérin, and M. Sergent, New Ternary Pnictides Ln_2NiX_2 (X = P, As) with a Filled Tip-Type Structure, *Mater. Res. Bull.*, 1988, **23**, p 891-898
55. B.M. Eisenmann, N; Mueller, W; Schaefer, H, Eine neue strukturelle Variante des BaAl4-Typs: Der $CaBe_2Ge_2$-Typ, *Zeitschrift für Naturforschung, Teil B: Anorganische Chemie, Organische Chemie, Biochemie, Biophysik, Biologie*, 1972, **27**, p 1155-1157
56. R. Shannon, Revised Effective Ionic Radii and Systematic Studies of Interatomic Distances in Halides and Chalcogenides, *Acta Crystallogr. Sect. A*, 1976, **32**, p 751-767
57. D. Fischer, B. Andriyevsky, and J.C. Schön, Systematics of the Allotrope Formation in Elemental Gallium Films, *Mater. Res. Express*, 2019, **6**, p 116401